Smart Structures and Systems, *Vol. 26, No. 5 (2020) 631-640*
DOI: https://doi.org/10.12989/sss.2020.26.5.631

On nonlinear vibration behavior of piezo-magnetic doubly-curved nanoshells

Sayed Sajad Mirjavadi[1], Hassan Bayani[2], Navid Khoshtinat[3], Masoud Forsat*[1], Mohammad Reza Barati[4] and A.M.S Hamouda[1]

[1]*Department of Mechanical and Industrial Engineering, Qatar University, P.O. Box 2713, Doha, Qatar*
[2]*Department of Electrical Engineering, Instituto Superior Técnico, UTL, Lisbon, Portugal*
[3]*Department of Mechanical Engineering, Science and Research Branch, Islamic Azad University, Tehran, Iran*
[4]*Fidar Project Qaem Company, Darvazeh Dolat, Tehran, Iran*

(*Received January 17, 2020, Revised July 19, 2020, Accepted July 31, 2020*)

Abstract. In this paper, nonlinear vibration behaviors of multi-phase Magneto-Electro-Elastic (MEE) doubly-curved nanoshells have been studied employing Jacobi elliptic function method. The doubly-curved nanoshell has been modeled by using nonlocal elasticity and classic shell theory. An exact estimation of nonlinear vibrational behavior of smart doubly-curved nanoshell has been obtained via Jacobi elliptic function method. This method can incorporate the influences of higher order harmonics leading to an exact estimation of nonlinear vibration frequency. It will be indicated that nonlinear vibrational frequency of doubly-curved nanoshell relies on nonlocal effect, material composition, curvature radius, center deflection and electro-magnetic field.

Keywords: doubly-curved shell; nonlinear vibration; Jacobi elliptic function; magneto-electro-elastic material; nonlocal elasticity

1. Introduction

An example for a smart material is piezoelectric-magnetic-elastic material in which magnetic-electric environments may lead to mechanical deformation (Aboudi 2001, Pan and Han 2005). This means that there is a coupling between magnetic-electric and elastic performances in such materials (Li and Shi 2009, Guo *et al*. 2016). In such materials, the material properties can be characterized by elastic, piezoelectric and magnetic constants. Structural components (beams, shells and plates) made of such smart materials are broadly utilized in actuators, sensors and intelligent systems. The material distribution in these structures may be homogenous or non-homogenous. When the material profile is variable thorough the thickness of a structure, the material distribution may be non-homogenous. As an example, a functional graded material is a non-homogenous material in which two materials are involved and all material properties change from one material to another. Based on the percentage and volume fraction of each material, the complete behavior of the structure can be defined. There are several investigations on smart piezoelectric-magnetic-elastic structures having functionally graded distribution (Kumaravel *et al*. 2007, Annigeri *et al*. 2007).

According to recent experiments and atomistic simulations, it is reported that the mechanical character of nano-size piezo-electric and piezo-magnetic structures are relied on small scale effects (Barati 2017, Yazid *et al*. 2018, Mokhtar *et al*. 2018, Ahmed *et al*. 2019, Al-Maliki *et al*. 2019, Fenjan *et al*. 2019). However, owning to the fact that classic continuum mechanical modelling is classified as a size free model, analyzing and investigating mechanical characteristics of small size structures based on the classic continuum theory yields inaccurate findings and accordingly wrongful designs. Howbeit, the atomistic modeling and molecular simulations are powerful tools for describing the size-dependent characteristics of small size structures, their application is not more economical because of the extra computational attempts. To prevail over such problems, a variety of size-dependent elasticity models including the nonlocal elasticity theory (Eringen 1972), strains gradient elasticity theory, refined couple stresses theory and etc., are established for incorporating small size effects via standardizing some scale parameters and have been broadly exerted for the designing and study of the mechanical character of micro or nano-structures (Thai and Vo 2012, Eltaher *et al*. 2012, Akbas 2016, Mouffoki *et al*. 2017, Bouafia *et al*. 2017, Mirjavadi *et al*. 2017a, b, 2018a, b, c, 2019a, b, c, Azimi 2017). The smart material discussed in previous paragraph has been extensively applied in nano-structures and nano-devices (Ke *et al*. 2014, Liu *et al*. 2018). However, at the nanoscale, the behavior of structure is dissimilar to macro scale counterparts. This is owning to the existence of small size effects. Such small size effects are incorporated in non-classical elasticity theories such as Eringen's theory which is also used by other authors.

Recently, several solution techniques have been developed for solving the nonlinear vibration equations of structural elements. Most studies give an approximate estimation of the vibrational behavior of structures (She *et*

*Corresponding author, Professor,
E-mail: masoudforsatlar@gmail.com

ISSN: 1738-1584 (Print), 1738-1991 (Online)

al. 2018, Alasadi *et al*. 2019). An exact solution of the cubic Duffing equation has been provided by Marinca and Herişanu (2011). Also, an exact traveling wave solution of the higher-order nonlinear Schrödinger equation for nonlinear dynamic analysis has been provided by Wang *et al*. (2016). Analytical insights into a generalized Semi-discrete system with time-varying coefficients by presenting exact solutions have been introduced by Zhang *et al*. (2020). Exact estimation of the vibrational behavior of structures can be obtained via Jacobi elliptic function method (Liu *et al*. 2001). This method can incorporate the influences of higher order harmonics leading to an exact estimation of nonlinear vibration frequency.

By using Jacobi elliptic function method, nonlinear vibration behaviors of multi-phase Magneto-Electro-Elastic (MEE) doubly-curved nanoshells have been studied. The doubly-curved nanoshell has been modeled by using nonlocal elasticity and classic shell theory. An exact estimation of nonlinear vibrational behavior of smart doubly-curved nanoshell has been obtained via Jacobi elliptic function method. It will be indicated that nonlinear vibrational frequency of doubly-curved nanoshell relies on nonlocal effect, material composition, curvature radius, center deflection and electro-magnetic field.

2. Theory of non-local elasticity for piezo-magnetic structures

According to the theory of non-local elasticity for smart magnetic-piezoelectric-elastic materials, stresses σ_{ij} electric displacement D_i and magnetic induction B_i can be defined in below form

$$\sigma_{ij} = \int_V \alpha(|x'-x|,\tau)\,[C_{ijkl}\varepsilon_{kl}(x') - e_{mij}E_m(x') - q_{nij}H_n(x')]dV(x') \quad (1a)$$

$$D_i = \int_V \alpha(|x'-x|,\tau)\,[e_{ikl}\varepsilon_{kl}(x') + s_{im}E_m(x') + d_{in}H_n(x')]dV(x') \quad (1b)$$

$$B_i = \int_V \alpha(|x'-x|,\tau)\,[q_{ikl}\varepsilon_{kl}(x') \quad (1c)$$

where V defines the volume. Above relations are associated with strains ε_{kl}, and electric-magnetic field (E_m, H_n). Till to now, mechanical analysis of piezo-magnetic nano-structures is performed based on diverse values for nonlocal parameter. Some of papers used actual value of nonlocal parameter with unit of *nm*, but some papers used normalized values for nonlocal factor in such a way that nonlocal parameter is normalized with respect to the length of nano-structure. Ke *et al*. (2014) and other authors used normalized values for nonlocal parameter as $\mu = e_0a/L = 0.1 \sim 0.3$ for studying vibrations of smart nanobeams with length L. Also, all components of stress field, electrical field displacement (D_i) and magnetic induction (B_i) for a size-dependent plate relevant to nonlocal theory may be written as

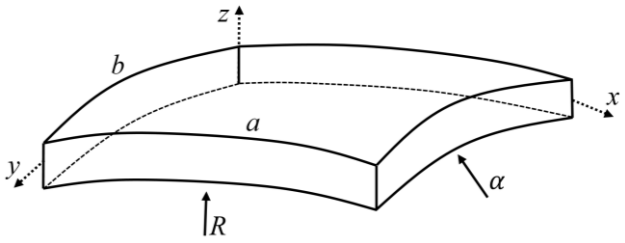

Fig. 1 A doubly-curved nanoshell

$$\sigma_{ij} - (e_0a)^2\nabla^2\sigma_{ij} = C_{ijkl}\varepsilon_{kl} - e_{mij}E_m - q_{nij}H_n \quad (2a)$$

$$D_i - (e_0a)^2\nabla^2 D_i = e_{ikl}\varepsilon_{kl} + s_{im}E_m + d_{in}H_n \quad (2b)$$

$$B_i - (e_0a)^2\nabla^2 B_i = q_{ikl}\varepsilon_{kl} + d_{im}E_m + \chi_{in}H_n \quad (2c)$$

where ∇^2 is the Laplacian operator.

3. MEE composites

A doubly-curved nanoshell of dimension a and b has been shown in Fig. 1. This doubly curved nanoshell is made of a MEE composite having two phases: a piezoelectric phase $BaTiO_3$ with volume fraction V_f and a magnetic phase $CoFe_2O_4$. All of material properties for the phases can be found in Table 1 which contains elastic (C_{ij}), piezoelectric (e_{ij}) and piezo-magnetic (q_{ij}) coefficients. Furthermore, k_{ij}, d_{ij} and x_{ij} respectively express dielectric, magnetic-electrical and magnetic permeability coefficients (Mirjavadi *et al*. 2020).

4. Shells made of multi-phase MEE material

By using thin shell theory for a doubly-curved nanoshell with curvatures (R, α), the three-dimensional displacement field which contains axial (u), circumferential (v) and transverse (w) components can be expressed as follows

$$u_1(x,y,z) = u(x,y) - \frac{z}{R}\frac{\partial w}{\partial x}(x,y) \quad (3)$$

$$u_2(x,y,z) = v(x,y) - \frac{z}{\alpha}\frac{\partial w}{\partial y}(x,y) \quad (4)$$

$$u_3(x,y,z) = w(x,y) \quad (5)$$

Above field components result in below relations foe the strain field

$$\varepsilon_{xx} = \frac{\partial u}{\partial x} - \frac{w}{R} - z\frac{\partial^2 w}{\partial x^2} + \frac{1}{2}\left(\frac{\partial w}{\partial x}\right)^2$$
$$\gamma_{xy} = \frac{\partial u}{\partial y} + \frac{\partial v}{\partial x} - 2z\frac{\partial^2 w}{\partial x \partial y} + \frac{\partial w}{\partial x}\frac{\partial w}{\partial y} \quad (6)$$

The induced electro-magnetic field having electric potential (Φ) and magnetic potential (Υ) to the doubly-

Table 1 Material properties of multi-phase MEE nanoshell made of $BaTiO_3$-$CoFe_2O_4$

Property	V_f = 0	V_f = 0.2	V_f = 0.4	V_f = 0.6	V_f = 0.8
C_{11} (GPa)	286	250	225	200	175
C_{13}	170	145	125	110	100
C_{33}	269.5	240	220	190	170
e_{31} (C/m^2)	0	-2	-3	-3.5	-4
e_{33}	0	4	7	11	14
q_{31} (N/Am)	580	410	300	200	100
q_{33}	700	550	380	260	120
k_{11} (10^{-9} C/Vm)	0.08	0.33	0.8	0.9	1
k_{33}	0.093	2.5	5	7.5	10
d_{11} (10^{-12} Ns/VC)	0	2.8	4.8	6	6.8
d_{33}	0	2000	2750	2500	1500
x_{11} (10^{-4} Ns^2/C^2)	-5.9	-3.9	-2.5	-1.5	-0.8
x_{33}	1.57	1.33	1	0.75	0.5
α_1 (10^{-6})	10	11.7	13	14.11	14.98
α_3	10	9.72	9.15	8.37	7.44

curved nano-scale shell can be expressed as

$$\Phi(x,y,z) = -\cos(\xi z)\phi(x,y) + \frac{2z}{h}V_E \tag{7}$$

$$\Upsilon(x,y,z) = -\cos(\xi z)\gamma(x,y) + \frac{2z}{h}\Omega \tag{8}$$

with $\xi = \pi/h$. Next, V_E and Ω define the exterior electrical voltages and magnetic potentials induced to the smart shell. All ingredients of electrical field (E_x, E_θ, E_z) and magnet field (H_x, H_θ, H_z) can be obtained as (Mirjavadi *et al*. 2020)

$$E_x = -\Phi_{,x} = \cos(\xi z)\frac{\partial \phi}{\partial x} \tag{9}$$

$$E_y = -\Phi_{,y} = \cos(\xi z)\frac{\partial \phi}{\partial y} \tag{10}$$

$$E_z = -\Phi_{,z} = -\xi \sin(\xi z)\phi - \frac{2V}{h} \tag{11}$$

$$H_x = -\Upsilon_{,x} = \cos(\xi z)\frac{\partial \gamma}{\partial x}, \tag{12}$$

$$H_y = -\Upsilon_{,y} = \cos(\xi z)\frac{\partial \gamma}{\partial y}, \tag{13}$$

$$H_z = -\Upsilon_{,z} = -\xi \sin(\xi z)\gamma - \frac{2\Omega}{h} \tag{14}$$

Knowing that *ea* is nonlocal parameter, Eq. (2) results in below field components for the doubly-curved nano-scale shell containing stain and electro-magnetic field.

$$(1-(ea)^2\nabla^2)\sigma_{xx} = \tilde{C}_{11}\varepsilon_{xx} + \tilde{C}_{12}\varepsilon_{yy} - \tilde{e}_{31}E_z - \tilde{q}_{31}H_z \tag{15}$$

$$(1-(ea)^2\nabla^2)\sigma_{yy} = \tilde{C}_{12}\varepsilon_{xx} + \tilde{C}_{11}\varepsilon_{yy} - \tilde{e}_{31}E_z - \tilde{q}_{31}H_z \tag{16}$$

$$(1-(ea)^2\nabla^2)\sigma_{x\theta} = \tilde{C}_{66}\gamma_{x\theta} \tag{17}$$

$$(1-(ea)^2\nabla^2)D_x = +\tilde{s}_{11}E_x + \tilde{d}_{11}H_x \tag{18}$$

$$(1-(ea)^2\nabla^2)D_y = +\tilde{s}_{11}E_\theta + \tilde{d}_{11}H_\theta \tag{19}$$

$$(1-(ea)^2\nabla^2)D_z = \tilde{e}_{31}\varepsilon_{xx} + \tilde{e}_{31}\varepsilon_{yy} + \tilde{s}_{33}E_z + \tilde{d}_{33}H_z \tag{20}$$

$$(1-(ea)^2\nabla^2)B_x = +\tilde{d}_{11}E_x + \tilde{\chi}_{11}H_x \tag{21}$$

$$(1-(ea)^2\nabla^2)B_y = +\tilde{d}_{11}E_\theta + \tilde{\chi}_{11}H_\theta \tag{22}$$

$$(1-(ea)^2\nabla^2)B_z = \tilde{q}_{31}\varepsilon_{xx} + \tilde{q}_{31}\varepsilon_{yy} + \tilde{d}_{33}E_z + \tilde{\chi}_{33}H_z \tag{23}$$

Reduced forms the constants C_{ij}, e_{ij} and q_{ij} can be found in the paper of Mirjavadi *et al*. (2020). Five governing equations for the doubly-curved MEE nanosehll can be expressed as

$$\frac{\partial N_{xx}}{\partial x} + \frac{\partial N_{xy}}{\partial y} = I_0\frac{\partial^2 u}{\partial t^2} - I_1\frac{\partial^3 w}{\partial x \partial t^2} \tag{24}$$

$$\frac{\partial N_{xy}}{\partial x} + \frac{\partial N_{yy}}{\partial y} = I_0\frac{\partial^2 v}{\partial t^2} - I_1\frac{\partial^3 w}{\partial y \partial t^2} \tag{25}$$

$$\begin{aligned}&\frac{\partial^2 M_{xx}}{\partial x^2} + 2\frac{\partial^2 M_{xy}}{\partial x \partial y} + \frac{\partial^2 M_{yy}}{\partial y^2} + \frac{N_{yy}}{\alpha} + \frac{N_{xx}}{R} + (N_{x0} + N_{xx})\\ &\left(\frac{\partial^2 w}{\partial x^2}\right) + \left(N_{y0} + N_{yy}\right)\left(\frac{\partial^2 w}{\partial y^2}\right) + 2N_{xy}\frac{\partial^2 w}{\partial x \partial y} =\\ &+ I_0\frac{\partial^2 w}{\partial t^2} + I_1\frac{\partial^3 u}{\partial x \partial t^2} + I_1\frac{\partial^3 v}{\partial y \partial t^2} - I_2\left(\frac{\partial^4 w}{\partial x^2 \partial t^2} + \frac{\partial^4 w}{\partial y^2 \partial t^2}\right)\end{aligned} \tag{26}$$

$$\int_{-h/2}^{h/2}\begin{pmatrix}\cos(\xi z)\dfrac{\partial D_x}{\partial x} + \cos(\xi z)\dfrac{\partial D_y}{\partial y}\\ +\xi \sin(\xi z)D_z\end{pmatrix}dz = 0 \tag{27}$$

$$\int_{-h/2}^{h/2}\begin{pmatrix}\cos(\xi z)\dfrac{\partial B_x}{\partial x} + \cos(\xi z)\dfrac{\partial B_y}{\partial y}\\ +\xi \sin(\xi z)B_z\end{pmatrix}dz = 0 \tag{28}$$

where $\{I_0, I_1, I_2\} = \int_{-h/2}^{h/2}\rho\{1, z, z^2\}dz$ are mass inertias. Also, note that N_{ij} and M_{ij} (ij = xx, xy, yy) describe membrane forces and bending moments

$$\begin{aligned}N_{xx} &= \int_{-h/2}^{h/2}(\sigma_{xx})dz\\ N_{xy} &= \int_{-h/2}^{h/2}(\sigma_{xy})dz\\ N_{yy} &= \int_{-h/2}^{h/2}(\sigma_{yy})dz\\ M_{xx} &= \int_{-h/2}^{h/2}z(\sigma_{xx})dz\end{aligned} \tag{29}$$

$$M_y = \int_{-h/2}^{h/2} z(\sigma_{yy})dz$$
$$M_{xy} = \int_{-h/2}^{h/2} z(\sigma_{xy})dz \tag{29}$$

Herein, this is supposed that the MEE nano-sized shell is affected by outer electrical voltages and magnetic potentials. Accordingly, N_{x0}, N_{y0} define the in-plane loading owning to external electrical voltages V and magnetic potentials Ω respectively and are defined as

$$N_{x0} = N_{y0} = N^E + N^H$$
$$N^E = -\int_{-h/2}^{h/2} \tilde{e}_{31}\frac{2V_E}{h}dz$$
$$N^H = -\int_{-h/2}^{h/2} \tilde{q}_{31}\frac{2\Omega}{h}dz \tag{30}$$

Based upon Hamilton's rule, it is feasible to express associated boundary conditions for MEE nano-scale shell based on n_x and n_y as cosines of directions

$$u = 0 \quad \text{or} \quad N_{xx}n_x + N_{xy}n_y = 0 \tag{31}$$

$$v = 0 \quad \text{or} \quad N_{xy}n_x + N_{yy}n_y = 0 \tag{32}$$

$$w = 0 \quad \text{or} \quad n_x\left(\frac{\partial M_{xx}}{\partial x} + \frac{\partial M_{xy}}{\partial y} - N_{x0}\frac{\partial w}{\partial x}\right) + n_y\left(\frac{\partial M_{yy}}{\partial y} + \frac{\partial M_{xy}}{\partial x} - N_{y0}\frac{\partial w}{\partial y}\right) = 0 \tag{33}$$

$$\frac{\partial w}{\partial x} = 0 \quad \text{or} \quad M_{xx}n_x + M_{xy}n_y = 0 \tag{34}$$

$$\frac{\partial w}{\partial y} = 0 \quad \text{or} \quad M_{xy}n_x + M_{yy}n_y = 0 \tag{35}$$

$$\phi = 0 \text{ or } \int_{-h/2}^{h/2}\left(cos(\xi z)D_x n_x + cos(\xi z)D_y n_y\right)dz = 0 \tag{36}$$

$$\gamma = 0 \text{ or } \int_{-h/2}^{h/2}\left(cos(\xi z)B_x n_x + cos(\xi z)B_y n_y\right)dz = 0 \tag{37}$$

Calculating the integrals presented in Eq. (29) gives the below relations for MEE nanoshells based upon nonlocal theory as

$$(1-(ea)^2\nabla^2)N_{xx} = A_{11}(\frac{\partial u}{\partial x} - \frac{w}{R} + \frac{1}{2}(\frac{\partial w}{\partial x})^2) - B_{11}\frac{\partial^2 w}{\partial x^2} + A_{12}(\frac{\partial v}{\partial y} - \frac{w}{\alpha} + \frac{1}{2}(\frac{\partial w}{\partial y})^2) - B_{12}\frac{\partial^2 w}{\partial y^2} + A_{31}^e\phi + A_{31}^m\gamma \tag{38}$$

$$(1-(ea)^2\nabla^2)M_{xx} = B_{11}(\frac{\partial u}{\partial x} - \frac{w}{R} + \frac{1}{2}(\frac{\partial w}{\partial x})^2) - D_{11}\frac{\partial^2 w}{\partial x^2} + B_{12}(\frac{\partial v}{\partial y} - \frac{w}{\alpha} + \frac{1}{2}(\frac{\partial w}{\partial y})^2) - D_{12}\frac{\partial^2 w}{\partial y^2} + E_{31}^e\phi + E_{31}^m\gamma \tag{39}$$

$$(1-(ea)^2\nabla^2)N_{yy} = A_{12}(\frac{\partial u}{\partial x} - \frac{w}{R} + \frac{1}{2}(\frac{\partial w}{\partial x})^2) - B_{12}\frac{\partial^2 w}{\partial x^2} + A_{11}(\frac{\partial v}{\partial y} - \frac{w}{\alpha} + \frac{1}{2}(\frac{\partial w}{\partial y})^2) - B_{11}\frac{\partial^2 w}{\partial y^2} + A_{31}^e\phi + A_{31}^m\gamma \tag{40}$$

$$(1-(ea)^2\nabla^2)M_{yy} = B_{12}(\frac{\partial u}{\partial x} - \frac{w}{R} + \frac{1}{2}(\frac{\partial w}{\partial x})^2) - D_{12}\frac{\partial^2 w}{\partial x^2} + B_{11}(\frac{\partial v}{\partial y} - \frac{w}{\alpha} + \frac{1}{2}(\frac{\partial w}{\partial y})^2) - D_{11}\frac{\partial^2 w}{\partial y^2} + E_{31}^e\phi + E_{31}^m\gamma \tag{41}$$

$$(1-(ea)^2\nabla^2)N_{x\theta} = A_{66}(\frac{\partial u}{\partial y} + \frac{\partial v}{\partial x} + \frac{\partial w}{\partial x}\frac{\partial w}{\partial y}) - 2B_{66}\frac{\partial^2 w}{\partial x\partial y} \tag{42}$$

$$(1-(ea)^2\nabla^2)M_{x\theta} = B_{66}(\frac{\partial u}{\partial y} + \frac{\partial v}{\partial x} + \frac{\partial w}{\partial x}\frac{\partial w}{\partial y}) - 2D_{66}\frac{\partial^2 w}{\partial x\partial y} \tag{43}$$

$$\int_{-\frac{h}{2}}^{\frac{h}{2}}(1-(ea)^2\nabla^2)D_x\, cos(\xi z)dz = +F_{11}^e\frac{\partial\phi}{\partial x} + F_{11}^m\frac{\partial\gamma}{\partial x} \tag{44}$$

$$\int_{-\frac{h}{2}}^{\frac{h}{2}}\left(1-(ea)^2\nabla^2\right)D_y\, cos(\xi z)dz = +F_{22}^e\frac{\partial\phi}{\partial y} + F_{22}^m\frac{\partial\gamma}{\partial y} \tag{45}$$

$$\int_{-h/2}^{h/2}(1-(ea)^2\nabla^2)D_z\xi\, sin(\xi z)dz = A_{31}^e(\frac{\partial u}{\partial x} - \frac{w}{R} + \frac{1}{2}(\frac{\partial w}{\partial x})^2) + A_{31}^e(\frac{\partial v}{\partial y} - \frac{w}{\alpha} + \frac{1}{2}(\frac{\partial w}{\partial y})^2) - E_{31}^e(\frac{\partial^2 w}{\partial x^2} + \frac{\partial^2 w}{\partial y^2}) - F_{33}^e\phi - F_{33}^m\gamma \tag{46}$$

$$\int_{-h/2}^{h/2}(1-(ea)^2\nabla^2)B_x\, cos(\xi z)dz = +F_{11}^m\frac{\partial\phi}{\partial x} + X_{11}^m\frac{\partial\gamma}{\partial x} \tag{47}$$

$$\int_{-h/2}^{h/2}(1-(ea)^2\nabla^2)B_y\, cos(\xi z)dz = +F_{22}^m\frac{\partial\phi}{\partial y} + X_{22}^m\frac{\partial\gamma}{\partial y} \tag{48}$$

$$\int_{-h/2}^{h/2}(1-(ea)^2\nabla^2)B_z\xi\, sin(\xi z)dz = A_{31}^m(\frac{\partial u}{\partial x} - \frac{w}{R} + \frac{1}{2}(\frac{\partial w}{\partial x})^2) + A_{31}^m(\frac{\partial v}{\partial y} - \frac{w}{\alpha} + \frac{1}{2}(\frac{\partial w}{\partial y})^2) - E_{31}^m(\frac{\partial^2 w}{\partial x^2} + \frac{\partial^2 w}{\partial y^2}) - F_{33}^m\phi - X_{33}^m\gamma \tag{49}$$

in which

$$\{A_{11}, B_{11}, D_{11}\} = \int_{-h/2}^{h/2}\tilde{C}_{11}\{1, z, z^2\}dz \tag{50}$$

$$\{A_{12}, B_{12}, D_{12}\} = \int_{-h/2}^{h/2} \tilde{C}_{12}\{1, z, z^2\} dz, \tag{51}$$

$$\{A_{66}, B_{66}, D_{66}\} = \int_{-h/2}^{h/2} \tilde{C}_{66}\{1, z, z^2\} dz, \tag{52}$$

$$\{A_{31}^e, E_{31}^e\} = \int_{-h/2}^{h/2} \tilde{e}_{31}\xi\, sin(\xi z)\{1, z\}\, dz \tag{53}$$

$$\{A_{31}^m, E_{31}^m\} = \int_{-h/2}^{h/2} \tilde{q}_{31}\xi\, sin(\xi z)\{1, z\}\, dz \tag{54}$$

$$\{F_{11}^e, F_{22}^e, F_{33}^e\} = \int_{-h/2}^{h/2} \{\tilde{s}_{11}\, cos^2(\xi z), \tilde{s}_{22}\, cos^2(\xi z), \tilde{s}_{33}\xi^2\, sin^2(\xi z)\} \tag{55}$$

$$\{F_{11}^m, F_{22}^m, F_{33}^m\} = \int_{-h/2}^{h/2} \{\tilde{d}_{11}\, cos^2(\xi z), \tilde{d}_{22}\, cos^2(\xi z), \tilde{d}_{33}\xi^2\, sin^2(\xi z)\}\, dz \tag{56}$$

$$\{X_{11}^m, X_{22}^m, X_{33}^m\} = \int_{-h/2}^{h/2} \{\tilde{\chi}_{11}\, cos^2(\xi z), \tilde{\chi}_{22}\, cos^2(\xi z), \tilde{\chi}_{33}\xi^2\, sin^2(\xi z)\} \tag{57}$$

The governing equations of thin MEE doubly-curved nanoshell based upon the displacement components and potential components might be achieved by placing Eqs. (38)-(49) into Eqs. (24)-(28) as

$$\begin{aligned} &A_{11}\left(\frac{\partial^2 u}{\partial x^2} - \frac{1}{R}\frac{\partial w}{\partial x} + \frac{\partial^2 w}{\partial x^2}\frac{\partial w}{\partial x}\right) - B_{11}\frac{\partial^3 w}{\partial x^3} + \\ &A_{66}\left(\frac{\partial^2 u}{\partial y^2} + \frac{\partial^2 v}{\partial x \partial y} + \frac{\partial^2 w}{\partial x \partial y}\frac{\partial w}{\partial y} + \frac{\partial w}{\partial x}\frac{\partial^2 w}{\partial y^2}\right) \\ &-2B_{66}\frac{\partial^3 w}{\partial x \partial y^2} + A_{31}^e\frac{\partial \phi}{\partial x} + A_{31}^m\frac{\partial \gamma}{\partial x} \\ &= (1 - (ea)^2\nabla^2)[I_0\frac{\partial^2 u}{\partial t^2} - I_1\frac{\partial^3 w}{\partial x \partial t^2}] \end{aligned} \tag{58}$$

$$\begin{aligned} &A_{66}\left(\frac{\partial^2 u}{\partial x \partial y} + \frac{\partial^2 v}{\partial x^2} + \frac{\partial^2 w}{\partial x^2}\frac{\partial w}{\partial y} + \frac{\partial w}{\partial x}\frac{\partial^2 w}{\partial x \partial y}\right) \\ &-2B_{66}\frac{\partial^3 w}{\partial x^2 \partial y} + A_{12}\left(\frac{\partial^2 u}{\partial x \partial y} - \frac{1}{R}\frac{\partial w}{\partial y} + \frac{\partial w}{\partial x}\frac{\partial^2 w}{\partial x \partial y}\right) \\ &-B_{12}\frac{\partial^3 w}{\partial x^2 \partial y} + A_{11}\left(\frac{\partial^2 v}{\partial y^2} - \frac{1}{\alpha}\frac{\partial w}{\partial y} + \frac{\partial^2 w}{\partial y^2}\frac{\partial w}{\partial y}\right) \\ &-B_{11}\frac{\partial^3 w}{\partial y^3} + A_{31}^e\frac{\partial \phi}{\partial y} + A_{31}^m\frac{\partial \gamma}{\partial y} \\ &= (1 - (ea)^2\nabla^2)[I_0\frac{\partial^2 v}{\partial t^2} - I_1\frac{\partial^3 w}{\partial y \partial t^2}] \end{aligned} \tag{59}$$

$$\begin{aligned} &B_{11}\left(\frac{\partial^3 u}{\partial x^3} - \frac{1}{R}\frac{\partial^2 w}{\partial x^2} + \frac{\partial^3 w}{\partial x^3}\frac{\partial w}{\partial x} + \frac{\partial^2 w}{\partial x^2}\frac{\partial^2 w}{\partial x^2}\right) \\ &-D_{11}\frac{\partial^4 w}{\partial x^4} - 2D_{12}\frac{\partial^4 w}{\partial x^2 \partial y^2} - 4D_{66}\frac{\partial^4 w}{\partial x^2 \partial y^2} - D_{11}\frac{\partial^4 w}{\partial y^4} \\ &+B_{12}\left(\frac{\partial^3 v}{\partial x^2 \partial y} - \frac{1}{\alpha}\frac{\partial^2 w}{\partial x^2} + \frac{\partial^3 w}{\partial x^2 \partial y}\frac{\partial w}{\partial y} + \frac{\partial^2 w}{\partial x \partial y}\frac{\partial^2 w}{\partial x \partial y}\right) \\ &+2B_{66}(\frac{\partial^3 u}{\partial x \partial y^2} + \frac{\partial^3 v}{\partial x^2 \partial y} + \frac{\partial^2 w}{\partial x^2}\frac{\partial^2 w}{\partial y^2} + \frac{\partial w}{\partial x}\frac{\partial^3 w}{\partial x \partial y^2} + \\ &\frac{\partial^3 w}{\partial x^2 \partial y}\frac{\partial w}{\partial y} + \frac{\partial^2 w}{\partial x \partial y}\frac{\partial^2 w}{\partial x \partial y}) + B_{12}\left(\frac{\partial^3 u}{\partial x \partial y^2} - \frac{1}{R}\frac{\partial^2 w}{\partial y^2}\right. \\ &\left.+\frac{\partial w}{\partial x}\frac{\partial^3 w}{\partial x \partial y^2}\right) + \frac{\partial^2 w}{\partial x \partial y}\frac{\partial^2 w}{\partial x \partial y}) + B_{11}(\frac{\partial^3 v}{\partial y^3} - \frac{1}{\alpha}\frac{\partial^2 w}{\partial y^2} \\ &+\frac{\partial^3 w}{\partial y^3}\frac{\partial w}{\partial y} + \frac{\partial^2 w}{\partial y^2}\frac{\partial^2 w}{\partial y^2}) + \frac{A_{11}}{R}(\frac{\partial u}{\partial x} - \frac{w}{R} + \frac{1}{2}(\frac{\partial w}{\partial x})^2) \\ &-\frac{B_{11}}{R}\frac{\partial^2 w}{\partial x^2} + \frac{A_{12}}{R}(\frac{\partial v}{\partial y} - \frac{w}{\alpha} + \frac{1}{2}(\frac{\partial w}{\partial y})^2) - \frac{B_{12}}{R}\frac{\partial^2 w}{\partial y^2} + \\ &\frac{A_{12}}{\alpha}(\frac{\partial u}{\partial x} - \frac{w}{R} + \frac{1}{2}(\frac{\partial w}{\partial x})^2) - \frac{B_{12}}{\alpha}\frac{\partial^2 w}{\partial x^2} + \frac{A_{11}}{\alpha}\left(\frac{\partial v}{\partial y} - \frac{w}{\alpha}\right. \\ &\left.+\frac{1}{2}\times(\frac{\partial w}{\partial y})^2\right) - \frac{B_{11}}{\alpha}\frac{\partial^2 w}{\partial y^2} + E_{31}^e(\frac{\partial^2 \phi}{\partial x^2} + \frac{\partial^2 \phi}{\partial y^2}) \\ &+\ E_{31}^m(\frac{\partial^2 \gamma}{\partial x^2} + \frac{\partial^2 \gamma}{\partial y^2}) + \frac{A_{31}^e}{\alpha}\phi + \frac{A_{31}^m}{\alpha}\gamma + \frac{A_{31}^e}{R}\phi \\ &+\frac{A_{31}^m}{R}\gamma + (1 - (ea)^2\nabla^2)(A_{11}(\frac{\partial u}{\partial x} - \frac{w}{R} + \frac{1}{2}(\frac{\partial w}{\partial x})^2)\right) \\ &-B_{11}\frac{\partial^2 w}{\partial x^2} + A_{12}\left(\frac{\partial v}{\partial y} - \frac{w}{\alpha} + \frac{1}{2}\times(\frac{\partial w}{\partial y})^2\right) - B_{12}\frac{\partial^2 w}{\partial y^2}) \\ &+A_{31}^e\phi + A_{31}^m\gamma)(\frac{\partial^2 w}{\partial x^2}) + 2(1 - (ea)^2\nabla^2)(A_{66}(\frac{\partial u}{\partial y} \\ &+\frac{\partial v}{\partial x} + \frac{\partial w}{\partial x}\frac{\partial w}{\partial y}) - 2B_{66}\frac{\partial^2 w}{\partial x \partial y})(\frac{\partial^2 w}{\partial x \partial y}) + (1 - (ea)^2 \\ &\nabla^2)(A_{12}(\frac{\partial u}{\partial x} - \frac{w}{R} + \frac{1}{2}(\frac{\partial w}{\partial x})^2) - B_{12}\frac{\partial^2 w}{\partial x^2} + A_{11} \\ &(\frac{\partial v}{\partial y} - \frac{w}{\alpha} + \frac{1}{2}(\frac{\partial w}{\partial y})^2) - B_{11}\frac{\partial^2 w}{\partial y^2} + A_{31}^e\phi + A_{31}^m\gamma) \\ &(\frac{\partial^2 w}{\partial y^2}) + (1 - (ea)^2\nabla^2)[-(N^E + N^H)(\frac{\partial^2 w}{\partial x^2} + \frac{\partial^2 w}{\partial y^2})] \\ &= (1 - (ea)^2\nabla^2)[+I_0\frac{\partial^2 w}{\partial t^2} + I_1\frac{\partial^3 u}{\partial x \partial t^2} + I_1\frac{\partial^3 v}{\partial y \partial t^2} \\ &- I_2(\frac{\partial^4 w}{\partial x^2 \partial t^2} + \frac{\partial^4 w}{\partial y^2 \partial t^2})] \end{aligned} \tag{60}$$

$$\begin{aligned} &+F_{11}^e\frac{\partial^2 \phi}{\partial x^2} + F_{11}^m\frac{\partial^2 \gamma}{\partial x^2} + F_{22}^e\frac{\partial^2 \phi}{\partial y^2} + F_{22}^m\frac{\partial^2 \gamma}{\partial y^2} \\ &+\ A_{31}^e(\frac{\partial u}{\partial x} - \frac{w}{R} + \frac{1}{2}(\frac{\partial w}{\partial x})^2 + \frac{\partial v}{\partial y} - \frac{w}{\alpha} + \frac{1}{2}(\frac{\partial w}{\partial y})^2) \\ &-\ E_{31}^e(\frac{\partial^2 w}{\partial x^2} + \frac{\partial^2 w}{\partial y^2}) - F_{33}^e\phi - F_{33}^m\gamma = 0 \end{aligned} \tag{61}$$

$$\begin{aligned} &+F_{11}^m\frac{\partial^2 \phi}{\partial x^2} + X_{11}^m\frac{\partial^2 \gamma}{\partial x^2} + F_{22}^m\frac{\partial^2 \phi}{\partial y^2} + X_{22}^m\frac{\partial^2 \gamma}{\partial y^2} \\ &+A_{31}^m(\frac{\partial u}{\partial x} - \frac{w}{R} + \frac{1}{2}(\frac{\partial w}{\partial x})^2 + \frac{\partial v}{\partial y} - \frac{w}{\alpha} + \frac{1}{2}(\frac{\partial w}{\partial y})^2) \\ &-\ E_{31}^m(\frac{\partial^2 w}{\partial x^2} + \frac{\partial^2 w}{\partial y^2}) - F_{33}^m\phi - X_{33}^m\gamma = 0 \end{aligned} \tag{62}$$

5. Solution of nonlinear governing equations

Based on Galerkin's method, it is possible to provide a solution for vibration problem of piezo-magnetic nanoshells based on the boundary conditions

on electric and magnetic $\phi = \gamma = 0$ displacements (63)

$$\text{on deflection } w = \frac{\partial^2 w}{\partial x^2} = 0 \quad (64)$$

In next step, the five variables based on thin piezo-magnetic shell model can be defined by

$$u = \sum_{m=1}^{\infty}\sum_{n=1}^{\infty} U_{mn}\bar{u}(x,y) = \sum_{m=1}^{\infty}\sum_{n=1}^{\infty} U_{mn}\frac{\partial X_m(x)}{\partial x}Y_n(y) \quad (65)$$

$$v = \sum_{m=1}^{\infty}\sum_{n=1}^{\infty} V_{mn}\bar{v}(x,y) = \sum_{m=1}^{\infty}\sum_{n=1}^{\infty} V_{mn}X_m(x)\frac{\partial Y_n(y)}{\partial y} \quad (66)$$

$$w = \sum_{m=1}^{\infty}\sum_{n=1}^{\infty} W_{mn}\bar{w}(x,y) = \sum_{m=1}^{\infty}\sum_{n=1}^{\infty} W_{mn}X_m(x)\,Y_n(y) \quad (67)$$

$$\phi = \sum_{m=1}^{\infty}\sum_{n=1}^{\infty} \Phi_{mn}\bar{\phi}(x,y) = \sum_{m=1}^{\infty}\sum_{n=1}^{\infty} \Phi_{mn}X_m(x)\,Y_n(y) \quad (68)$$

$$\gamma = \sum_{m=1}^{\infty}\sum_{n=1}^{\infty} \Upsilon_{mn}\bar{\gamma}(x,y) = \sum_{m=1}^{\infty}\sum_{n=1}^{\infty} \Upsilon_{mn}X_m(x)\,Y_n(y) \quad (69)$$

where maximum amplitudes are defined as: U_{mn}, V_{mn}, W_{mn}, Φ_{mn} and Υ_{mn}. Test functions X_m and Y_n should be chosen in proper formation to capture the impacts of boundary condition when two edges are Simply-Supported (S-S)

$$X_m = sin(\frac{m\pi}{a}x) \quad (70)$$

$$Y_n = sin(\frac{n\pi}{b}y) \quad (71)$$

Considering Galerkin's approach and placing displacement variables presented by Eqs. (65)-(69) into Eqs. (58)-(62) yields the following ordinary nonlinear governing equations as

$$k_{11}U + k_{21}V + k_{31}W + n_1W^2 + k_{41}\Phi + k_{51}\Upsilon = 0 \quad (72)$$

$$k_{12}U + k_{22}V + k_{32}W + n_2W^2 + k_{42}\Phi + k_{52}\Upsilon = 0 \quad (73)$$

$$\begin{aligned} &M\ddot{W} + k_{13}U + k_{23}V + k_{33}W + n_3W^2 + n_4W^3 \\ &+ n_5UW + n_6VW + k_{43}\Phi + k_{53}\Upsilon + n_9\Phi W \\ &+ n_{10}\Upsilon W = 0 \end{aligned} \quad (74)$$

$$k_{14}U + k_{24}V + k_{34}W + n_7W^2 + k_{44}\Phi + k_{54}\Upsilon = 0 \quad (75)$$

$$k_{15}U + k_{25}V + k_{35}W + n_8W^2 + k_{45}\Phi + k_{55}\Upsilon = 0 \quad (76)$$

in which n_i and k_{ij} are the components of nonlinear and linear stiffness matrices and M is mass matrix.

Due to the fact that there are five coupled nonlinear governing equations, presenting a closed-form of vibration frequency as a function of maximum amplitude (W) is very difficult. Here, with the help of simultaneously solving of Eqs. (72), (73), (75) and (76), it is possible to find amplitudes (U, V, Φ, Υ) as functions of transverse amplitude or maximum deflection (W). However, obtained amplitude have very complicated forms and it is not possible to provide a closed-form for them. So, for simplicity they are defined in new form as

$$\begin{aligned} U &\to \hat{U}(W) \\ V &\to \hat{V}(W) \\ \Phi &\to \hat{\Phi}(W) \\ \Upsilon &\to \hat{\Upsilon}(W) \end{aligned} \quad (77)$$

Then, obtained amplitude are inserted into Eq. (74) in order to find a single nonlinear governing equation for nanoshell as

$$\begin{aligned} &k_{13}\hat{U} + k_{23}\hat{V} + k_{33}W + n_3W^2 + n_4W^3 \\ &+ n_5\hat{U}W + n_6\hat{V}W + k_{43}\hat{\Phi} + k_{53}\hat{\Upsilon} + n_9\hat{\Phi}W \\ &+ n_{10}\hat{\Upsilon}W + M\ddot{W} = 0 \end{aligned} \quad (78)$$

It finally reduces to

$$\ddot{W} + \frac{K_1}{M}W + \frac{K_2}{M}W|W| + \frac{K_3}{M}W^3 = 0 \quad (79)$$

It should be noted that for considering the oscillations in both positive and negative directions it is considered that $W^2 = W|W|$. Note that K_1, K_2 and K_3 have complex forms due to the reason discussed above Eq. (77) and it is not possible to express their closed forms. Based on the initial conditions $W = \bar{W}, \dot{W} = 0$ at $t = 0$, Exact solution of above equation can be introduced based on Jacobi elliptic function (cn) as

$$W = \bar{W}cn(\omega t, k^2) \quad (80)$$

Note that k^2 is the modulus of the elliptic function; $\bar{W}$ is vibration amplitude. It should be pointed out that ω is the frequency of elliptic function. Based on the Fourier expansion, the Jacobi elliptic function (cn) can be expressed as a series of corresponding trigonometric function as

$$cn(\omega t, k^2) = \frac{2\pi}{kK}\sum_{r=0}^{\infty}\frac{q^{r+\frac{1}{2}}}{1+q^{2r+1}}cos\left((2r+1)\frac{\pi\omega t}{2K}\right) \quad (81)$$

where $K(k)$ is the complete elliptic integral of the first kind; $q = exp(-\pi K'/K)$ and $K' = K(l)$ is the associated complete elliptic integral of the first kind. Note that $l = \sqrt{1-k^2}$ is the complementary modulus. The whole procedure of obtaining vibration frequency can be found in the paper of Mirjavadi *et al*. (2020) knowing that the vibration frequency (ψ) depends on the period of elliptic function, $\psi = 2\pi/T$ in which

$$T = \frac{4K(k)}{\omega} \quad (82)$$

Also, some normalized parameters can be introduced in this paper such as

Table 2 Validation of vibration frequency for a nonlocal MEE nanoshell

	μ = 0		μ = 0.02		μ = 0.03	
	Ke *et al*. (2014)	Present	Ke *et al*. (2014)	Present	Ke *et al*. (2014)	Present
L/R = 30	0.1935	0.1935	0.1657	0.1657	0.1435	0.1435
L/R = 40	0.1662	0.1662	0.1296	0.1296	0.1062	0.1062
L/R = 50	0.1578	0.1578	0.1114	0.1114	0.0874	0.0874

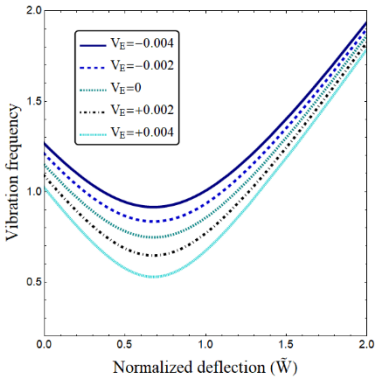

Fig. 2 Vibration frequency curves of the nano-size shell against non-dimension amplitude for diverse electrical voltage (a = 40 h, R = 7a, μ = 0.2, Ω = 0, V_f = 20%)

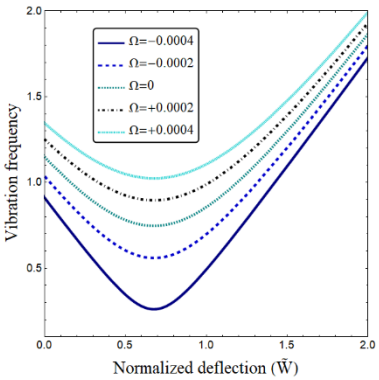

Fig. 3 Vibration frequency curves of the nano-size shell against non-dimension amplitude for diverse magnetic field intensities (V_f = 20%, μ = 0.2, V_E = 0)

$$\varpi = 10\psi L\sqrt{\frac{\rho}{C_{11}}}$$
$$\mu = \frac{ea}{a} \tag{83}$$
$$\widetilde{W} = \frac{\bar{W}}{h}$$

6. Results and discussions

In this chapter, impacts of different factors such as magneto-electrical field, nonlocality, curvature radius and material compositions on nonlinear vibrational frequencies

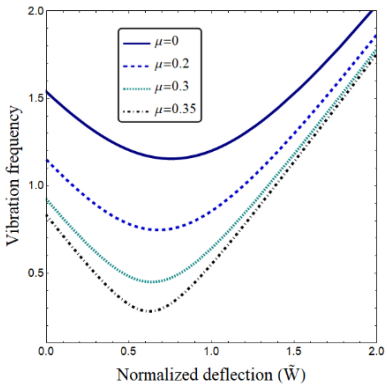

Fig. 4 Vibration frequency curves of the nano-size shell against non-dimension amplitude for diverse nonlocal factors (V_f = 20%, V_E = 0, Ω = 0)

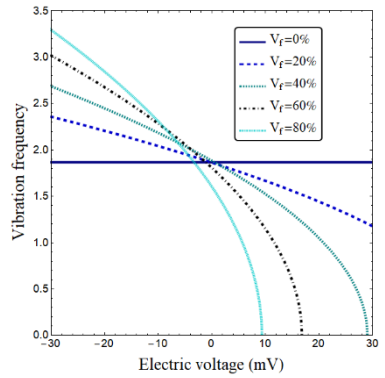

Fig. 5 Vibration frequency against applied voltage accounting for diverse volume fractions of piezoelectric phase (μ = 0.2, Ω = 0, W/h = 2)

of doubly-curved MEE nanoshells have been examined. The thickness of nano-sized shell has been chosen to be h = 1 nm. For the confirmation purpose, nonlinear vibrational frequencies have been compared with those of MEE cylindrical nanoshell presented by Ke *et al*. (2014) and a worthy agreement is found according to the findings represented in Table 2.

In Figs. 2 and 3, changing of non-dimension vibration frequency of doubly-curved MEE nanoshell versus non-dimension amplitude is illustrated for different electrical voltages and magnetic potentials when a = 40 h and μ = 0.2. This is deduced that non-dimension vibration frequencies of doubly-curved MEE nano-size shell are significantly influenced by the magnitude and sign of magnetic and electric potentials for each values of non-dimension amplitude. It is concluded that negative magnitudes for

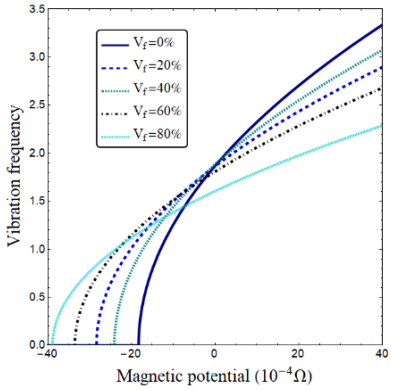

Fig. 6 Vibration frequency against magnetic potential accounting for diverse volume fractions of piezoelectric phase (μ = 0.2, V_E = 0, W/h = 2)

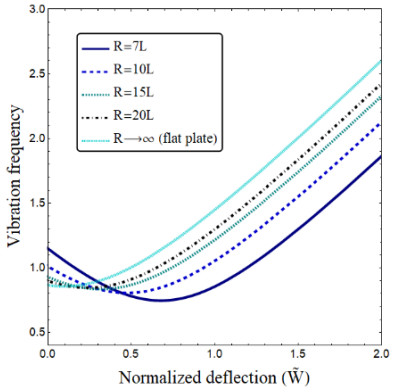

Fig. 7 Vibration frequency against normalized deflection accounting for diverse curvature radius (V_f = 20%, V_E = 0, Ω = 0)

magnetic potentials give lower vibration frequency than positive magnetic intensity factor. While, smaller magnitudes of electrical voltages result in greater vibration frequency. Actually, the imposed negative/positive magnetic intensities might generate the in-plane compressive and tensile forces. Whereas, electrical fields show an opposite influence. It is also found that the vibration frequency begins to decline with the increase of non-dimension amplitude. Next, the vibration frequency begins to increase at larger values of non-dimension amplitude.

Fig. 4 illustrates the variations of non-dimension vibration frequency of doubly-curved MEE nanoshell against non-dimension amplitude, for different nonlocal factors when V_E = 0 and V_f = 20%. This is deduced that non-dimension vibration frequencies of nonlocal doubly-curved MEE nano-size shell are often lower than that of local macro-size shell. Vibration frequencies decrease by the increment of the nonlocal factor at a fixed magnetic intensity and electrical voltage. This incident is because of the reason that the low size impacts, that describe the reciprocal influences of every points within the area, might decline the strength of the nano-size structure.

Fig. 5 depicts vibrational frequency variation versus electrical voltage accounting for different volume fractions of piezoelectric constituent (V_f = 0, 20%, 40%, 60% and 80%). For simplicity, the nonlocal scale factor is set as μ = 0.2. The variation of applied electric voltage is considered between V_E = -30 mV and V_E = +30 mV. During this range of electric voltage it is found that the vibration frequency has a reducing trend. At certain values of positive applied voltages, the nonlinear vibration frequency becomes zero. This is owning to the reason that positive voltages induce compressive in-plane load to MEE nanoshell leading to lower structural stiffness. In these values of electrical voltage, the nanoshell will buckle and vibration frequency is zero.

Vibrational frequency variation versus magnetic field intensity (Ω) accounting for different volume fractions of piezoelectric constituent has been plotted in Fig. 6. For simplicity, the nonlocal scale factor is set as μ = 0.2. The variation of magnetic field intensity is considered between $\Omega = -40 \times 10^{-4}$ and $\Omega = +40 \times 10^{-4}$. During this range of magnetic field intensity it is found that the vibration frequency has an increasing trend. At special values of negative magnetic field intensity, the nonlinear vibration frequency is zero and buckling of the nanoshell occurs. The most important observation from the figure is that vibrational frequency increases with lower rates as the piezoelectric constituent percentage increases. This is because at higher values of piezoelectric constituent percentage the nanoshell is less sensitive to magnetic field.

Vibrational frequency versus normalized deflection of the nanoshell accounting for different curvature radius has been plotted in Fig. 7. Note that an infinite curvature radius results in frequency curves for flat plates. So, as the value of curvature has been reduced, the curvature radius has more announced effect on frequency curves.

7. Conclusions

Vibration characteristics of a piezo-magnetic nanoshell with double curvature were reported in the present article. The complete formulation and solution for the problem based on thin shell model was presented. There was no change in vibration frequency versus applied voltage when the piezoelectric volume fraction was zero. Also, applying positive or negative magnetic potentials led to increasing or reducing the vibration frequency. Also, this was reported that the vibration behavior of the nano-sized shell is sensitive to material composition. Another observation was that size effects due to nonlocality changed significantly the vibration behaviors of piezo-magnetic nano-sized shell. Also, the dependency of vibration frequency on negative and positive voltages was clearly explained. Also, as the value of curvature was reduced, the curvature radius had more announced effect on frequency curves.

Acknowledgements

The authors would like to thank FPQ (Fidar project Qaem) for providing the fruitful and useful help.

References

Aboudi, J. (2001), "Micromechanical analysis of fully coupled electro-magneto-thermo-elastic multiphase composites", *Smart Mater. Struct.*, **10**(5), 867. https://doi.org/10.1088/0964-1726/10/5/303.

Ahmed, R.A., Fenjan, R.M. and Faleh, N.M. (2019), "Analyzing post-buckling behavior of continuously graded FG nanobeams with geometrical imperfections", *Geomech. Eng., Int. J.*, **17**(2), 175-180. https://doi.org/10.12989/gae.2019.17.2.175.

Akbaş, Ş.D. (2016), "Forced vibration analysis of viscoelastic nanobeams embedded in an elastic medium", *Smart Struct. Syst., Int. J.*, **18**(6), 1125-1143. http://dx.doi.org/10.12989/sss.2016.18.6.1125.

Al-Maliki, A.F., Faleh, N.M. and Alasadi, A.A. (2019), "Finite element formulation and vibration of nonlocal refined metal foam beams with symmetric and non-symmetric porosities", *Struct. Monit. Maint., Int. J.*, **6**(2), 147-159. https://doi.org/10.12989/smm.2019.6.2.147.

Alasadi, A.A., Ahmed, R.A. and Faleh, N.M. (2019), "Analyzing nonlinear vibrations of metal foam nanobeams with symmetric and non-symmetric porosities", *Adv. Aircr. Spacecr. Sci., Int. J.*, **6**(4), 273-282. https://doi.org/10.12989/aas.2019.6.4.273.

Annigeri, A.R., Ganesan, N. and Swarnamani, S. (2007), "Free vibration behaviour of multiphase and layered magneto-electro-elastic beam", *J. Sound Vib.*, **299**(1-2), 44-63. https://doi.org/10.1016/j.jsv.2006.06.044.

Azimi, M., Mirjavadi, S.S., Shafiei, N. and Hamouda, A.M.S. (2017), "Thermo-mechanical vibration of rotating axially functionally graded nonlocal Timoshenko beam", *Appl. Phys. A*, **123**(1), 104. https://doi.org/10.1007/s00339-016-0712-5.

Barati, M.R. (2017), "Coupled effects of electrical polarization-strain gradient on vibration behavior of double-layered flexoelectric nanoplates", *Smart Struct. Syst., Int. J.*, **20**(5), 573-581. https://doi.org/10.12989/sss.2017.20.5.573.

Bouafia, K., Kaci, A., Houari, M.S.A., Benzair, A. and Tounsi, A. (2017), "A nonlocal quasi-3D theory for bending and free flexural vibration behaviors of functionally graded nanobeams", *Smart Struct. Syst., Int. J.*, **19**(2), 115-126. https://doi.org/10.12989/sss.2017.19.2.115.

Eltaher, M.A., Emam, S.A. and Mahmoud, F.F. (2012), "Free vibration analysis of functionally graded size-dependent nanobeams", *Appl. Math. Comput.*, **218**(14), 7406-7420. https://doi.org/10.1016/j.amc.2011.12.090.

Eringen, A.C. (1972), "Linear theory of nonlocal elasticity and dispersion of plane waves", *Int. J. Eng. Sci.*, **10**(5), 425-435. https://doi.org/10.1016/0020-7225(72)90050-X.

Eshraghi, I., Jalali, S.K. and Pugno, N.M. (2016), "Imperfection sensitivity of nonlinear vibration of curved single-walled carbon nanotubes based on nonlocal timoshenko beam theory", *Materials*, **9**(9), 786. https://doi.org/10.3390/ma9090786.

Fenjan, R.M., Ahmed, R.A., Alasadi, A.A. and Faleh, N.M. (2019), "Nonlocal strain gradient thermal vibration analysis of double-coupled metal foam plate system with uniform and non-uniform porosities", *Coupled Syst. Mech., Int. J.*, **8**(3), 247-257. https://doi.org/10.12989/csm.2019.8.3.247.

Guo, J., Chen, J. and Pan, E. (2016), "Static deformation of anisotropic layered magnetoelectroelastic plates based on modified couple-stress theory", *Compos. Part B Eng.*, **107**, 84-96. https://doi.org/10.1016/j.compositesb.2016.09.044.

Ke, L.L., Wang, Y.S., Yang, J. and Kitipornchai, S. (2014), "The size-dependent vibration of embedded magneto-electro-elastic cylindrical nanoshells", *Smart Mater. Struct.*, **23**(12), 125036. https://doi.org/10.1088/0964-1726/23/12/125036.

Kumaravel, A., Ganesan, N. and Sethuraman, R. (2007), "Buckling and vibration analysis of layered and multiphase magneto-electro-elastic beam under thermal environment", *Multidiscip. Model. Mater. Struct.*, **3**(4), 461-476. https://doi.org/10.1163/157361107782106401.

Li, Y. and Shi, Z. (2009), "Free vibration of a functionally graded piezoelectric beam via state-space based differential quadrature", *Compos. Struct.*, **87**(3), 257-264. https://doi.org/10.1016/j.compstruct.2008.01.012.

Liu, S., Fu, Z., Liu, S. and Zhao, Q. (2001), "Jacobi elliptic function expansion method and periodic wave solutions of nonlinear wave equations", *Phys. Lett. A*, **289**(1-2), 69-74. https://doi.org/10.1016/S0375-9601(01)00580-1.

Liu, H., Liu, H. and Yang, J. (2018), "Vibration of FG magneto-electro-viscoelastic porous nanobeams on visco-Pasternak foundation", *Compos. Part B Eng.*, **155**, 244-256. https://doi.org/10.1016/j.compositesb.2018.08.042.

Mahmoudi, A., Benyoucef, S., Tounsi, A., Benachour, A., Adda Bedia, E.A. and Mahmoud, S.R. (2019), "A refined quasi-3D shear deformation theory for thermo-mechanical behavior of functionally graded sandwich plates on elastic foundations", *J. Sandw. Struct. Mater.*, **21**(6), 1906-1929. https://doi.org/10.1177%2F1099636217727577.

Marinca, V. and Herişanu, N. (2011), "Explicit and exact solutions to cubic Duffing and double-well Duffing equations", *Math. Comput. Model.*, **53**(5-6), 604-609. https://doi.org/10.1016/j.mcm.2010.09.011.

Mirjavadi, S.S., Matin, A., Shafiei, N., Rabby, S. and Mohasel Afshari, B. (2017a), "Thermal buckling behavior of two-dimensional imperfect functionally graded microscale-tapered porous beam", *J. Therm. Stress.*, **40**(10), 1201-1214. https://doi.org/10.1080/01495739.2017.1332962.

Mirjavadi, S.S., Rabby, S., Shafiei, N., Afshari, B.M. and Kazemi, M. (2017b), "On size-dependent free vibration and thermal buckling of axially functionally graded nanobeams in thermal environment", *Appl. Phys. A*, **123**(5), 315. https://doi.org/10.1007/s00339-017-0918-1.

Mirjavadi, S.S., Afshari, B.M., Barati, M.R. and Hamouda, A.M.S. (2018a), "Strain gradient based dynamic response analysis of heterogeneous cylindrical microshells with porosities under a moving load", *Mater. Res. Express*, **6**(3), 035029. https://doi.org/10.1088/2053-1591/aaf5a2.

Mirjavadi, S.S., Afshari, B.M., Khezel, M., Shafiei, N., Rabby, S. and Kordnejad, M. (2018b), "Nonlinear vibration and buckling of functionally graded porous nanoscaled beams", *J. Braz. Soc. Mech. Sci. Eng.*, **40**(7), 352. https://doi.org/10.1007/s40430-018-1272-8.

Mirjavadi, S.S., Mohasel Afshari, B., Shafiei, N., Rabby, S. and Kazemi, M. (2018c), "Effect of temperature and porosity on the vibration behavior of two-dimensional functionally graded micro-scale Timoshenko beam", *J. Vib. Control*, **24**(18), 4211-4225. https://doi.org/10.1177%2F1077546317721871.

Mirjavadi, S.S., Afshari, B.M., Barati, M.R. and Hamouda, A.M.S. (2019a), "Nonlinear free and forced vibrations of graphene nanoplatelet reinforced microbeams with geometrical imperfection", *Microsyst. Technol.*, **25**(8), 3137-3150. https://doi.org/10.1007/s00542-018-4277-4.

Mirjavadi, S.S., Afshari, B.M., Barati, M.R. and Hamouda, A.M.S. (2019b), "Transient response of porous inhomogeneous nanobeams due to various impulsive loads based on nonlocal strain gradient elasticity", *Int. J. Mech. Mater. Des.*, **2019**, 1-12. https://doi.org/10.1007/s10999-019-09452-2.

Mirjavadi, S.S., Forsat, M., Nikookar, M., Barati, M.R. and Hamouda, A.M.S. (2019c), "Nonlinear forced vibrations of sandwich smart nanobeams with two-phase piezo-magnetic face sheets", *Eur. Phys. J. Plus*, **134**(10), 508. https://doi.org/10.1140/epjp/i2019-12806-8.

Mirjavadi, S.S., Forsat, M., Badnava, S., Barati, M.R. and Hamouda, A.M.S. (2020), "Nonlinear dynamic characteristics of nonlocal multi-phase magneto-electro-elastic nano-tubes with

different piezoelectric constituents", *Appl. Phys. A*, **126**(8), 1-16. https://doi.org/10.1007/s00339-020-03743-8.

Mohammadi, H., Mahzoon, M., Mohammadi, M. and Mohammadi, M. (2014), "Postbuckling instability of nonlinear nanobeam with geometric imperfection embedded in elastic foundation", *Nonlin. Dyn.*, **76**(4), 2005-2016. https://doi.org/10.1007/s11071-014-1264-x.

Mohammadimehr, M. and Alimirzaei, S. (2016), "Nonlinear static and vibration analysis of Euler-Bernoulli composite beam model reinforced by FG-SWCNT with initial geometrical imperfection using FEM", *Struct. Eng. Mech., Int. J.*, **59**(3), 431-454. http://dx.doi.org/10.12989/sem.2016.59.3.431.

Mokhtar, Y., Heireche, H., Bousahla, A.A., Houari, M.S.A., Tounsi, A. and Mahmoud, S.R. (2018), "A novel shear deformation theory for buckling analysis of single layer graphene sheet based on nonlocal elasticity theory", *Smart Struct. Syst., Int. J.*, **21**(4), 397-405. https://doi.org/10.12989/sss.2018.21.4.397.

Mouffoki, A., Bedia, E.A., Houari, M.S.A., Tounsi, A. and Mahmoud, S.R. (2017), "Vibration analysis of nonlocal advanced nanobeams in hygro-thermal environment using a new two-unknown trigonometric shear deformation beam theory", *Smart Struct. Syst., Int. J.*, **20**(3), 369-383. https://doi.org/10.12989/sss.2017.19.2.115.

Pan, E. and Han, F. (2005), "Exact solution for functionally graded and layered magneto-electro-elastic plates", *Int. J. Eng. Sci.*, **43**(3-4), 321-339. https://doi.org/10.1016/j.ijengsci.2004.09.006.

She, G.L., Yuan, F.G., Ren, Y.R., Liu, H.B. and Xiao, W.S. (2018), "Nonlinear bending and vibration analysis of functionally graded porous tubes via a nonlocal strain gradient theory", *Compos. Struct.*, **203**, 614-623. https://doi.org/10.1016/j.compstruct.2018.07.063.

Thai, H.T. and Vo, T.P. (2012), "A nonlocal sinusoidal shear deformation beam theory with application to bending, buckling, and vibration of nanobeams", *Int. J. Eng. Sci.*, **54**, 58-66. https://doi.org/10.1016/j.ijengsci.2012.01.009.

Wang, H., Chen, L., Liu, H. and Zheng, S. (2016), "Nonlinear dynamics and exact traveling wave solutions of the higher-order nonlinear Schrödinger equation with derivative non-kerr nonlinear terms", *Math. Probl. Eng.*, **2016**, 7405141. https://doi.org/10.1155/2016/7405141.

Yazid, M., Heireche, H., Tounsi, A., Bousahla, A.A. and Houari, M.S.A. (2018), "A novel nonlocal refined plate theory for stability response of orthotropic single-layer graphene sheet resting on elastic medium", *Smart Struct. Syst., Int. J.*, **21**(1), 15-25. https://doi.org/10.12989/sss.2018.21.1.015.

Zhang, S., Zhao, S. and Xu, B. (2020), "Analytical insights into a generalized semidiscrete system with time-varying coefficients: Derivation, exact solutions and nonlinear soliton dynamics", *Complexity*, **2020**, 1543503. https://doi.org/10.1155/2020/1543503.

CC